(Deoxycholic acid)$_2$:Ferrocene: A Phase Transition Determined by the Dynamic Behavior of the Included Guest Molecules

Matthias Müller,[†] Alison J. Edwards,[†] Keith Prout,*[,†] W. Mark Simpson,[‡] and Stephen J. Heyes*[,‡]

Chemical Crystallography Laboratory, Department of Chemistry, University of Oxford, 9 Parks Road, Oxford OX1 3PD, United Kingdom, and the Inorganic Chemistry Laboratory, Department of Chemistry, University of Oxford, South Parks Road, Oxford OX1 3QR, United Kingdom

Received October 18, 1999. Revised Manuscript Received January 26, 2000

The deoxycholic acid inclusion complex (DCA)$_2$:ferrocene (**1**) undergoes a "gradual" phase transition above ambient temperature, "completed" by ∼360 K. The phase transition is characterized by using single-crystal X-ray diffraction and ^{13}C CP/MAS NMR spectroscopy. ^{13}C CP/MAS NMR spectra of **1** suggest two DCA molecules in the crystallographic unit cell, which on heating become increasingly similar, until beyond ∼345 K only one molecular type is detected. The crystal structure has been determined at 360, 294, 200, and 100 K. Single-crystal diffraction data show a similar phase change at around 350 K. At $T \leq 294$ K the structure is solved in $P2_12_12_1$, and at 360 K, the *a* axis is halved in a high-temperature form with symmetry $P22_12_1$. In the temperature region 320−340 K, the single-crystal X-ray diffraction structure cannot be solved adequately. The atomic displacement ellipsoids of the ferrocene molecule at the various temperatures are consistent with a wobble about the molecular 5-fold axis proposed previously from ^{2}H NMR studies. The transition, although most clearly observed in the positions of the deoxycholic acid molecules, is largely dominated by the dynamic behavior of the included guest ferrocene molecules. The mechanistic nature of and the similarities and differences in the way this transition is detected by NMR and XRD techniques are discussed.

Introduction

Host and guest molecules of molecular inclusion adducts exert an influence on the structural and dynamical properties of each other. It is becoming increasingly apparent that the delicate balance of forces in such materials leads to exceptional variability in structure, dynamics, polymorphism, and phase transitions in response to changes in external conditions,[1,2] and wide-ranging applications have been proposed for inclusion systems for these reasons. X-ray diffraction (XRD) is typically the method of choice for determining the 3D structure of such crystalline compounds,[3] as it is sensitive to the long-range ordering of the host molecules. Guest molecules, however, are often subject to static or dynamic disorder, and in such cases, only space- and time-averaged atomic coordinates may be determined. Solid-state NMR spectroscopy reports on local structures and is sensitive directly to the dynamics of molecules over a wide range of time scales.[4] The combination of XRD and NMR is synergic, allowing characterization of these materials[5,6] in substantially more detail than is possible from the simple summation of information from each individual technique in isolation. The findings reported here form part of a series of studies on the molecular motion and disorder of guest molecules of different shape and symmetry in the host cavities of 3α,-12α-dihydroxy-5β-cholan-24-oic acid [deoxycholic acid (DCA), Figure 1]. The DCA host structures are based on corrugated sheets of DCA molecules H-bonded head-to-tail, extending in two dimensions, and stacked so as to leave channels. These channels are typically filled with guest molecules that often are disordered.[7]

The published X-ray structure[8] for (DCA)$_2$:Fe(C$_5$H$_5$)$_2$ (**1**) reports that the asymmetric unit contains one DCA molecule and half a ferrocene molecule, the iron atom of which is on the crystallographic 2-fold axis of space

* To whom correspondence should be addressed.
[†] Chemical Crystallography Laboratory.
[‡] Inorganic Chemistry Laboratory.

(1) Atwood, J. L.; Davies, J. E. D.; McNicol, D. D., Eds. *Inclusion Compounds*; Academic Press: London, 1984; Vols. 1−3; OUP: Oxford, 1991; Vols. 4 and 5
(2) Dunitz, J. D. *Acta Crystallogr.* **1995**, *B51*, 619−631. Dunitz, J. D. *Pure Appl. Chem.* **1991**, *63*, 177−185.
(3) Dunitz, J. D. *X-ray Analysis and the Structure of Organic Molecules*, 2nd ed., 2nd repr.; VCH: Weinheim, 1995.
(4) Muetterties, E. L. *Inorg. Chem.* **1965**, *4*, 769−771.
(5) Fattah, J.; Twyman, J. M.; Heyes, S. J.; Watkin, D. J.; Edwards, A. J.; Prout, K.; Dobson, C. M. *J. Am. Chem. Soc.* **1993**, *115*, 5636−5650.
(6) Brouwer, E. B.; Ripmeester, J. A.; Enright, G. D. *J. Inclusion Phenom. Mol. Recognit. Chem.* **1996**, *24*, 1−17. McGeorge, G.; Harris, R. K.; Batsanov, A. S.; Churakov, A. V.; Chippendale, A. M.; Bullock, J. F.; Gan, Z. H. *J. Phys. Chem. A* **1998**, *102*, 3505−3513.
(7) Giglio, E. In *Inclusion Compounds*; Atwood, J. L., Davies, J. E. D., MacNicol, D. D., Eds.; Academic Press: London, 1984; Vol. 2, pp 207−229.
(8) Miki, K.; Kasai, N.; Tsutsumi, H.; Miyata, M.; Takemoto, K. *J. Chem. Soc. Chem. Commun.* **1987**, 545−546.

10.1021/cm990654a CCC: $19.00
Published on Web 04/09/2000

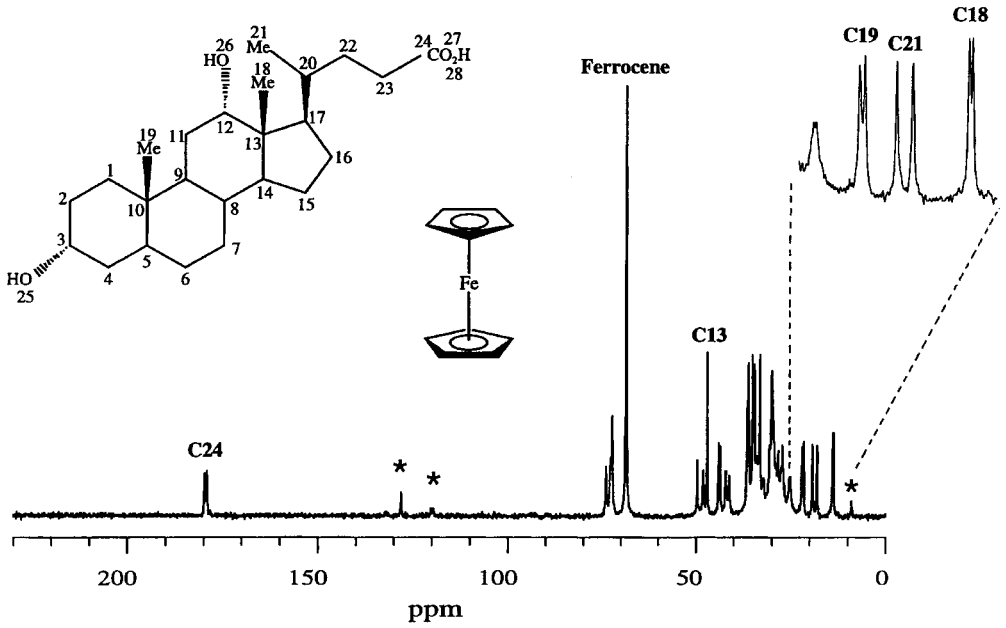

Figure 1. The complete ^{13}C CP/MAS NMR spectrum for (DCA)$_2$:ferrocene (**1**) at 297 K together with the structural formula and atom numbering (MAS rate = 3 kHz; the asterisk (*) indicates a spinning sideband).

group $P22_12_1$. In contrast, the reported ambient temperature ^{13}C CP/MAS NMR spectrum of **1**[9,10] indicates the resonances of the DCA methyl carbon atoms to be 1:1 "doublets". This implies two inequivalent DCA molecules in the crystallographic asymmetric unit. The solid-state ^{2}H NMR spectra of the complex with perdeuterioferrocene, reported for the temperature range 200−350 K, can be simulated on a model of a fast limit ($>10^8$ s^{-1}) motion of the ferrocene.[9] This motion was deconvoluted into a libration about the 5-fold axis together with a lower amplitude cylindrically symmetric "wobble" of that axis, both increasing in amplitude with increasing temperature. Wide line ^{1}H second moment and spin−lattice relaxation studies[11] in the range 100−400 K have been interpreted in respect of cyclopentadienyl ring reorientation with a low activation barrier, 180° jumps of ferrocene molecules about a 2-fold axis at higher temperatures and finally "proton-exchange" within the hydrogen bonds between DCA molecules. ^{57}Fe Mössbauer studies of **1**[12] suggest "cone-like" precession of the ferrocene molecules, which is considered from the decreased quadrupolar splitting to show increased amplitude with increased temperature. The combined evidence of the studies above indicate such a large increase with temperature in the molecular motion of the ferrocene that it might be expected to lead to a phase change. The complex **1** was therefore investigated using variable-temperature ^{13}C CP/MAS NMR and variable-temperature, single-crystal X-ray diffraction to attempt to resolve the crystallographic dilemma and pursue further the nature of the motional behavior of the ferrocene.

Experimental Section

1. Preparation and Characterization. 1 was prepared and characterized by the methods described in ref 9.

2. Solid-State ^{13}C CP/MAS NMR. Spectra were acquired on a Bruker MSL 200 spectrometer equipped with an Oxford Instruments 4.7 T wide-bore (98 mm) superconducting solenoid magnet, operating at a frequency of 50.32 MHz for ^{13}C. CP/MAS spectra were recorded using a multinuclear, proton-enhanced, double-bearing magic-angle sample spinning probe (Bruker Z32-DR-MAS-7DB), utilizing dry nitrogen for all gas requirements. Approximately 300 mg of sample was packed into 7 mm zirconia rotors with Kel-F or BN caps, for MAS at 3 kHz. A single contact cross-polarization pulse sequence was used with alternate cycle spin temperature inversion and proton flip-back. A rotationally asynchronous TPPI phase-sensitive CP/MAS 2D-exchange NMR experiment, consisting of 1024 increments of 62 μs in t_1 and a mixing time of 1 s was performed as described by Twyman and Dobson.[13] Full experimental procedures including temperature calibration are detailed in ref 14.

Spectral fits to Voigt line shapes were performed with the use of a suite of macros developed for the IGOR computer program[15] running on an Apple Macintosh computer. Each calculation was performed in the same manner and was repeated with a wide range of initial NMR fitting parameters. First a section of baseline was selected and was fitted to a third-order polynomial function. The baseline parameters were then fixed and the experimental data were fitted to a selected number of Voigt line shapes. Finally all of the constraints were released and a full fit was attempted.

3. Single-Crystal X-ray Diffraction Structure Determinations. Three different diffractometers of Enraf Nonius manufacture were used to record single-crystal diffraction data, a CAD4 serial diffractometer, a FAST area detector system, and a DIP2020 image plate.

The FAST used a crystal cooler by Molecular Structure Corp. and the DIP 2020 an Oxford Cryosystems CRYOSTREAM cooling system. Data from the FAST was processed

(9) Heyes, S. J.; Dobson, C. M. *Magn. Reson. Chem.* **1990**, *28*, 37−46.
(10) Imashiro, F.; Kitazaki, N.; Kuwahara, D.; Nakai, T.; Terao, T. *J. Chem. Soc., Chem. Commun.* **1991**, 85−86.
(11) Narankevich, Z.; Blyumenfeld, A. L.; Sokolov, V. I. *Bull. Russ. Acad. Sci. − Div. Chem. Sci.* **1992**, *41*, 462−467.
(12) Nakashita, M.; Sakai, H. *Chem. Lett.* **1996**, 927−928.
(13) Twyman, J. M.; Dobson, C. M. *Magn. Reson. Chem.* **1990**, *28*, 163−170.
(14) Edwards, A. J.; Burke, N. J.; Dobson, C. M.; Prout, C.; Heyes, S. J. *J. Am. Chem. Soc.* **1995**, *117*, 4637−4653.
(15) IGOR, Wavemetrics Inc.; http://www.wavemetrics.com/.

with the MADNES[16] program suite and from the DIP2000 with the HKL (DENZO and SCALEPACK)[17] program suite. Lorentz and polarization corrections were applied and an absorption correction except in the case of the area detector systems. However, in the latter a partial absorption correction is implicit in the interframe scaling. The structures were solved by direct methods using the program SIR92,[18] which located all non-hydrogen atoms. The hydrogen atoms were located in difference electron density syntheses, but were placed geometrically. A "robust resistant"[19] Chebychev polynomial[20] weighting scheme was applied. All Fourier calculations and subsequent least-squares refinements were carried out using the CRYSTALS[21] program. Atomic scattering factors were taken from *International Tables for X-ray Crystallography*.[22] Details of the structure analyses, the final atomic coordinates, and anisotropic displacement parameters are to be found in Tables S1−S4 of the Supporting Information.

4. Differential Scanning Calorimetry (DSC). Thermogravimetric analysis (TGA) and DSC were performed simultaneously with a Rheometric Scientific STA-1500H thermal analyzer. Ten milligrams of sample was heated and cooled in a static air atmosphere between 293 and 393 K at a rate of 2°/min and the thermal cycle was repeated twice in succession.

Results

1. ^{13}C CP/MAS NMR Spectra. ^{13}C CP/MAS NMR spectra were recorded over the temperature range 260−360 K. The extremely high resolution ($\Delta\nu_{1/2} \approx 9-15$ Hz) ambient temperature spectrum is shown in Figure 1, as partially assigned in ref 9. The most significant region for monitoring crystallographic details of the structure (12−24 ppm) contains pairs of lines for each of the methyl groups C19, C21 and C18 of DCA, which is consistent with *two* crystallographically distinct DCA molecules in the asymmetric unit of the crystal. These methyl groups are situated on the periphery of the molecule and are expected to be especially sensitive to changes in local environment.[23] The variation of this region of the spectrum with temperature, which is fully reversible, is followed in Figure 2. As the temperature is increased these resonances, which at 297 K are sharp ($\Delta\nu_{1/2} \approx 9$ Hz) with large splittings, gradually broaden slightly, the two component peaks of each "doublet" move progressively together, each eventually "coalescing" to a single resonance (as broad as $\Delta\nu_{1/2} \approx 20$ Hz) which sharpens again at the highest temperatures studied. Thus, the high-temperature (>345 K) spectrum shows only one resonance for each of the methyl groups. This suggests that a transformation has occurred to give a high-temperature phase with only one DCA molecule

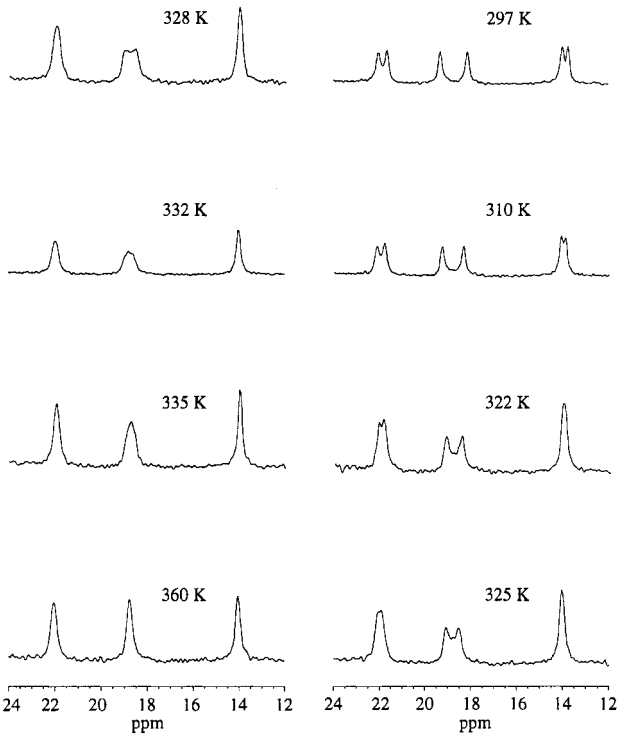

Figure 2. Methyl region of the ^{13}C CP/MAS NMR spectra of $(DCA)_2$:ferrocene (**1**) at selected temperatures.

in the crystallographic asymmetric unit. The transformation appears to occur gradually over the wide temperature range of ~305−350 K and is fully reversible. Hysteresis is not detected in the NMR spectra recorded on cooling the sample back to ambient temperature. This interpretation is in conflict with the previous single-crystal X-ray diffraction structure.[8] Thus, the X-ray diffraction of crystals of **1** was reexamined, first to resolve the question of the content of the asymmetric unit and second to search for diffraction evidence for a phase change above ambient temperature.

2. Single-Crystal X-ray Diffraction Structure Determinations. Three sets of single crystal X-ray diffraction measurements were carried out. A selected crystal was mounted on an Enraf Nonius CAD4 diffractometer and the orientation matrix and cell dimensions determined from 25 well-centered reflections following the manufacturer's recommended procedures. These results appeared to confirm those reported previously and so were in conflict with the ^{13}C CP/MAS NMR results. To accommodate two DCA molecules in the asymmetric unit, either the crystal is monoclinic or the unit cell is doubled in volume. An examination of the Laue symmetry did not favor the former. The apparent orthorhombic space group was $P22_12_1$ but DCA complexes in space group $P2_12_12_1$ with the *a* axis doubled are known.[24−27] Closer investigation of the diffraction pattern on the supposition of a doubled *a* axis showed that there were weak reflections *hkl*, with $h = 2n + 1$.

(16) Pflugrath, J.; Messerschmidt, A. MADNES, Munich Area Detector (New EEC) System, version EEC11/09/89, with enhancements by Enraf-Nonius Corp., Delft, The Netherlands.

(17) Gewirth, D. *The HKL Manual*, written with the cooperation of the program authors Z. Otwinowski and W. Minor; Yale University, 1995.

(18) Altomare, A.; Cascarano, G.; Giacovazzo, G.; Guagliardi, A.; Burla, M. C.; Polidori, G.; Camalli, M. *J. Appl. Crystallogr.* **1994**, *27*, 435−436.

(19) Prince, E. *Mathematical Techniques in Crystallography and Material Sciences*; Springer-Verlag Inc.: New York, 1982.

(20) Carruthers, J. R.; Watkin, D. J. *Acta Crystallogr., Sect. A* **1979**, *A35*, 698−699.

(21) Watkin, D. J.; Prout, C. K.; Carruthers, J. R.; Betteridge; P. W. *CRYSTALS Issue 10*; Chemical Crystallography Laboratory, University of Oxford: Oxford, 1996.

(22) Wilson, A. J. C., Ed. *International Tables for Crystallography*, Kluwer Academic Publishers: Dordrecht, 1995; Vol. C (Repr. With Corr.).

(23) Fyfe, C. A. *Solid State NMR for Chemists*; C. F. C. Press: Guelph, 1993; pp 284−286.

(24) Coiro, V. M.; Mazza, F.; Pochetti, G.; Giglio, E. *Acta Crystallogr., Sect. A* **1984,** *40*, C273. Coiro, V. M.; Mazza, F.; Pochetti, G.; Giglio, E.; Pavel, N. V. *Acta Crystallogr., Sect. C* **1985**, *41*, 229−232.

(25) Coiro, V. M.; Giglio, E.; Mazza, F.; Pavel, N. V. *J. Inclusion Phenom.* **1984**, *1*, 329−337.

(26) Popovitz-Biro, R.; Tang, C. P.; Chang, H. C.; Lahav, M.; Leiserowitz, L. *J. Am. Chem. Soc.* **1985**, *107*, 4043−4058.

(27) D'Andrea, A.; Fedeli, W.; Giglio, E.; Mazza, F.; Pavel N. V. *Acta Crystallogr., Sect. B* **1981**, *37*, 368−372.

Table 1. Variation of Unit Cell Dimensions of (DCA)$_2$:Fe(C$_5$H$_5$)$_2$ (1) with Temperature, As Measured on the DIP2000 Diffractometer[a]

T, K	*a*, Å	*b*, Å	*c*, Å
294	14.116(1)	13.650(1)	27.236(1)
305	14.29(1)	13.78(2)	27.55(3)
315	14.38(1)	13.85(1)	27.71(4)
320	14.47(1)	14.02(2)	26.54(4)
325	14.46(1)	13.99(2)	26.63(1)
330	14.45(1)	13.84(2)	27.82(4)
340	14.38(1)	13.76(2)	26.46(4)
350	7.30(1)	14.11(4)	26.52(6)
360	7.127(1)	13.687(1)	27.301(1)

[a] Those at 294 and 360 K are measured using a full 90 frames. The rest are obtained from single frames and are more approximate, but serve to show the temperature at which the indexing of the diffraction pattern no longer requires the doubled *a* axis.

A full data set was collected and the structure solved and refined in $P2_12_12_1$.

The experiments were repeated with an Enraf-Nonius FAST area detector diffractometer at 293, 248, 198, and 148 K. The structure was solved and refined at each temperature in $P2_12_12_1$ with consistent unit cell dimensions (2.7% contraction from 293 to 148 K).

The Oxford Cryosystems CRYOSTREAM variable-temperature system together with the Enraf-Nonius DIP2000 image plate made possible diffraction measurements above ambient temperature and thus investigation of the possible phase change suggested by the ^{13}C CP/MAS NMR experiments. A crystal was mounted with its *a* axis approximately parallel to the axis of rotation of the diffractometer so that the images approximated to *a* axis oscillation diffractograms. Single frame images were recorded at 5° intervals from 305 to 330 K and at 340, 350, and 360 K. The crystal was recooled to 294 K and a full diffraction pattern recorded and then reheated to 360 K and the full diffraction pattern was collected. At 294 K, there were 2518 observed ($I > 3\sigma I$) reflections for $h = 2n$ with an average intensity of 10.33 on the arbitrary F_o scale and 2258 reflections for $h = 2n + 1$ with an average intensity of 5.86 on the same arbitrary scale. At 360 K, there was no observable diffraction intensity at the reciprocal lattice points corresponding to $h = 2n + 1$ for the low-temperature unit cell. The reflections *hkl* with $h = 2n + 1$ are clearly visible up to 340 K, but have disappeared by 350 K. The images recorded at 305−315 K were indexed readily, with excellent agreement between the observed and calculated positions of the diffraction maxima, on the larger $P2_12_12_1$ unit cell. From 320 to 340 K, a satisfactory fit could not be obtained. At 350 K, a reasonable fit was obtained with the *a* axis half its former value, and at 360 K, excellent agreement was obtained. The values obtained for the unit cell dimensions using the DENZO program[17] are given in Table 1. The structure was solved and refined at 294 K in space group $P2_12_12_1$ and at 360 K in space group $P22_12_1$. The DIP2000 has no facility for recording intensity check reflections but a comparison of the diffraction intensities of equivalent frames before and after the temperature cycling experiments suggested that there had been a 10% loss of intensity. Therefore, to record the diffraction pattern at 200 and 100 K another crystal of near identical dimensions was selected. The crystal data and other details of these four structure analyses performed with the DIP2000 Instrument are reported in Table 2.

The diffraction data confirm that the crystals undergo a gradual phase change on heating, as suggested by the ^{13}C CP/MAS NMR spectra. However, the apparent temperature at which the two techniques indicate the phase change to be "completed" is not the same. The NMR data suggest completion of the phase change by ∼340 K but X-ray diffraction indicates apparently minor changes in this region and that the major events take place between 340 and 350 K, where the NMR spectra show more minor changes.

The X-ray crystal structures at 100, 200, and 294 K are of the same phase and are virtually identical. For direct comparison with the published structure,[8] the

Table 2. Crystal Data Recorded Using the DIP2000 Diffractometer Together with Selected Details of the Data Collections and Structure Refinements

	T, K			
	100	200	294	360
formula	$C_{58}H_{90}FeO_8$			
M_r	971.20			
crystal size	0.3 × 0.3 × 0.4			
crystal system	orthorhombic			
space group	$P2_12_12_1$	$P2_12_12_1$	$P2_12_12_1$	$P22_12_1$
a, Å	13.928(1)	14.010(1)	14.116(1)	7.127(1)
b, Å	13.559(1)	13.603(1)	13.650(1)	13.687(1)
c, Å	27.027(1)	27.158(1)	27.236(1)	27.301(1)
V,Å^3	5104	5176	5247	2663
Z	4	4	4	2
radiation wavelength, Å	0.71069 (Mo K$_\alpha$)			
ρ_{Calc}, Mg m^{-3}	1.26	1.25	1.23	1.21
μ, cm^{-1}	3.46	3.42	3.37	3.32
θ_{min}, θ_{max}, deg	1, 26			
h_{min}, h_{max}	0, 17	0, 17	0, 16	0, 8
k_{min}, k_{max}	0, 17	0, 17	0, 17	0, 17
l_{min}, l_{max}	−33, 0	−34, 0	34, 0	0, 34
measured data	50365	51287	52303	27355
unique data	5820	5930	5785	3884
obs data ($I > 3\sigma(I)$)	5316	5249	4776	2406
no. of parameters refined	622	628	628	315
resid. electron density (e Å^{-3})	−0.46, 0.40	−0.24, 0.41	−0.32, 0.91	−0.32, 0.36
R	0.051	0.048	0.063	0.061
R_w	0.057	0.057	0.075	0.082

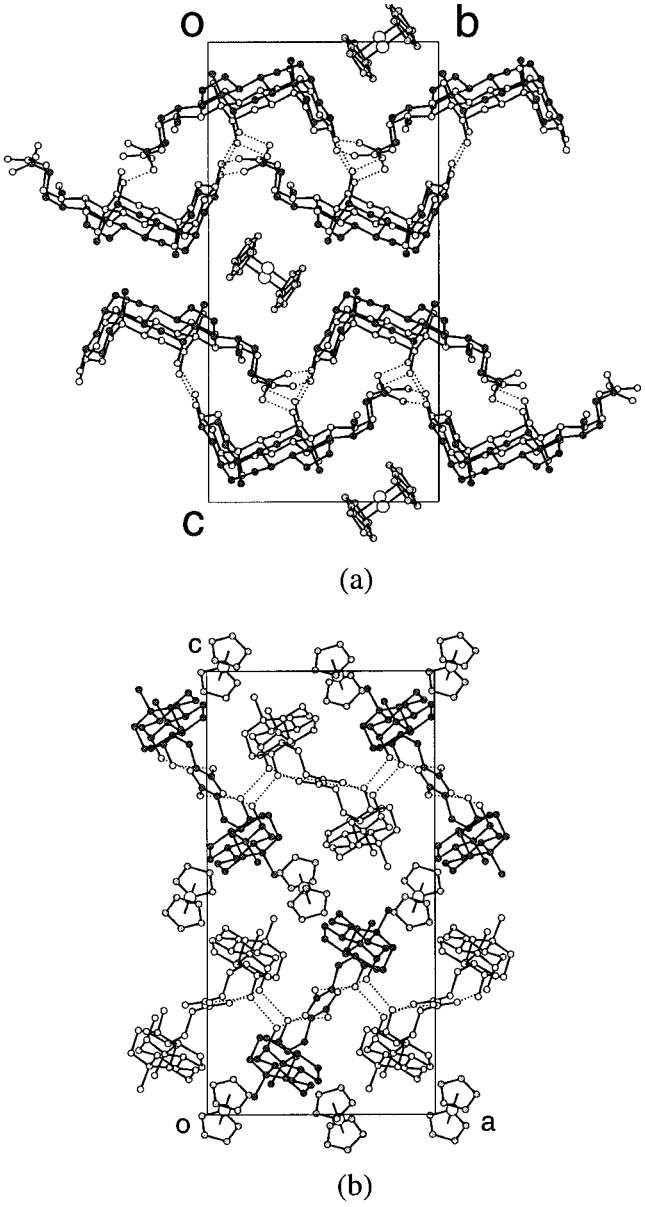

Figure 3. Packing diagram of $(DCA)_2$:ferrocene (**1**) at 100 K; the hydrogen bonds are represented by dotted lines: (a) viewed along *a* and (b) viewed along *b*.

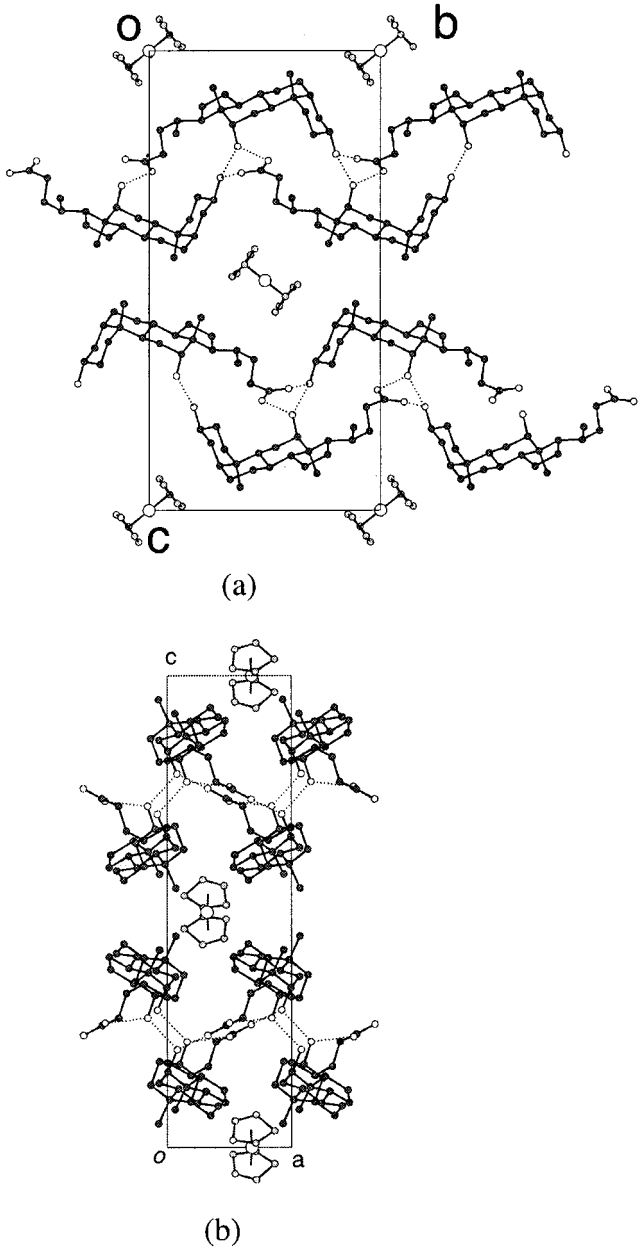

Figure 4. Packing diagram of $(DCA)_2$:ferrocene (**1**) at 360 K; the hydrogen bonds are represented by dotted lines: (a) viewed along *a* and (b) viewed along *b*.

structure at 294 K is shown in Figure 3. The DCA molecules form H-bonded layers parallel to the *ab* plane. These layers have the same structure as that found in the $(DCA)_2$:(guest) complexes with pinacolone,[24] quadricyclane,[25] cyclohexanone,[26] and norbornadiene.[27] Each DCA layer contains both of the crystallographically distinct DCA molecules (the open and filled circles in Figure 3) in a similar orientation, but one with a small shift in the *c* axis direction with respect to the other. The layers come together to form a structure with channels parallel to the *a* axis. At intervals, these channels open out to form approximately spherical cavities where well-ordered ferrocene guest molecules are located. In the solid-state NMR experiment, the differentiation of the two crystallographically distinct DCA molecules in the low temperature form concentrated on the methyl groups at C18, C19, and C21. The methyl groups C21 are differentiated in the crystal structure by the different conformations of the carboxylic acid side chain of which they form part (see Figure 3a). The methyl groups C18 and C19 can be identified in Figure 3b and are to the left of the ferrocene molecule in the center of the diagram in projection, pointing into the ferrocene containing channel. The ferrocene appears to be displaced toward the DCA represented with black circles. In the high-temperature structure, the side chains containing C21 are identical by symmetry and the ferrocene is placed symmetrically in the channels with respect to C18 and C19.

The high temperature form (360 K), Figure 4, has the structure $P22_12_1$, as reported previously for the room temperature form[8] and the same as for the ambient temperature forms of $(DCA)_2$·*d*-camphor[28] and $(DCA)_2$·*l*-camphor.[29] The small *z* shift that distinguishes the

(28) Jones, J. G.; Schwarzbaum, S.; Lessinger, L. *Acta Crystallogr., Sect. B* **1982**, *38*, 1207−1215.
(29) Candeloro De Sanctis, S.; Coiro, V. M.; Mazza, F.; Pochetti, G. *Acta Crystallogr., Sect. B* **1995**, *51*, 81−89.

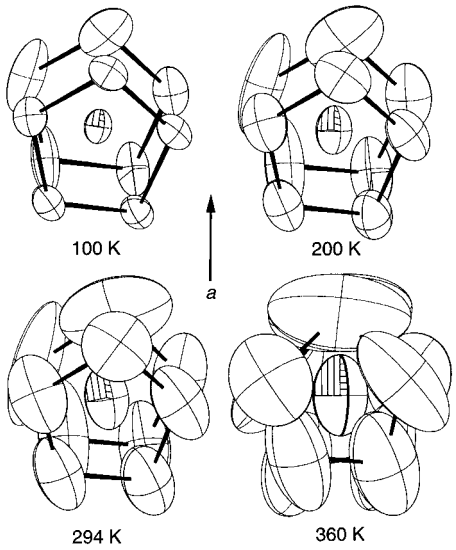

Figure 5. Thermal ellipsoids of the ferrocene guest molecules of (DCA)$_2$:ferrocene (**1**) at 100 K, 200, 294, and 360 K; the *a* direction is lying in the plane of the paper as indicated; the C_5H_5 rings of the 360 K structure are related by a crystallographic C_2 axis.

crystallographically distinct DCA molecules in the $P2_12_12_1$ structure has disappeared, the DCA molecules viewed down *a* are superposed, and the iron atoms of the ferrocene lie on the 2-fold symmetry axes so that the cyclopentadienyl groups of a ferrocene molecule are equivalent by symmetry. The anisotropic displacement parameters (adps) indicate that the DCA host is remarkably rigid and well-resolved for such a high temperature.

3. Atomic Displacement Parameters. The adps of the ferrocene molecules at 100, 200, 294, and 360 K, Figure 5, show them to be well-defined, with relatively restricted, highly anisotropic vibrational freedom. The adps of each atom have the same shape and are oriented in the same way at the different temperatures and in the data from three different diffractometers. It is therefore reasonable to suggest that they reflect the thermal motion of the atoms and are not determined by experimental errors such as absorption problems or incorrect weighting. In the low-temperature form, the adps of the two crystallographically independent cyclopentadienyl rings of the ferrocene in the $P2_12_12_1$ structure are of different amplitude. The maximum movement is in the *z* direction within the DCA cavities (Figure 3). The adps are consistent both with a libration of the essentially rigid ferrocene molecules about their 5-fold axes and an effective libration of each 5-fold axis. The second libration motion appears to be pivoted near the center of one of the rings, not at the iron atom as might perhaps have been expected, and this is confirmed by TLS analysis[30] using the ANISO routine in the CRYSTALS program.[21] This can be rationalized by examining non-hydrogen contacts that are smaller than 4 Å for the ferrocene molecules with the DCA channel, which number 11 for the ring at the librational pivot, and only 7 for the ring which is displaced further in the libration. Variable-temperature solid-state ^{2}H NMR experiments[9] suggest that the motion of the ferrocene molecule can be described in terms of a libration about the 5-fold axis plus a wobble of that axis, and this is consistent with the observed adps. The NMR line shapes were however unable to show that the librational pivot point was not at the iron atom position, but actually closer to one of the cyclopentadienyl rings. The adps for the two cyclopentadienyl rings of a ferrocene molecule in the 360 K structure are identical, due to their crystallographic equivalence.

4. Differential Scanning Calorimetry (DSC). The DSC trace of **1** on heating and cooling between 293 and 393 K shows a gradual change in the gradient between 293 and 360 K without hysteresis, but is effectively constant in the range 360−393 K. There is no distinct endo- or exothermic event detected at any temperature. The phase transformation detected by NMR and X-ray Diffraction can therefore be regarded as a second-order transition on Ehrenfest's thermodynamic classification.[31]

Discussion of the Nature of the Phase Transition

The phase change is viewed as a gradual progression from an ordered low-temperature phase to a disordered or partially disordered high-temperature phase. Looking down the guest channels in the low-temperature form, the centers of the guest cavities alternate from side to side of the 2-fold screw axis. The methyl groups C18, C19, and C21 of the two crystallographically distinct DCA molecules are environmentally inequivalent and have different chemical shifts in the NMR. On heating, thermal agitation of the ferrocene molecules results in greater equivalence of the DCA molecules over the temperature range of the phase change and shifts the centers of the cavities closer together until they coincide eventually on a 2-fold axis. The target methyl groups become crystallographically equivalent and have the same NMR chemical shift. It might have been imagined that in the high-temperature form thermal agitation would dynamically shift the cavities from side to side of the 2_1 axis so that on average the cavity is centered on the 2-fold axis. However, comparison of the adps in the X-ray structures for the DCA atoms, which are always relatively small, and for the ferrocene atoms, which increase progressively with temperature, shows that spatially extensive dynamic events are restricted to the ferrocene molecules. Thus, it is believed that there is a dynamic disorder of the ferrocene molecules.

The apparent eclipsed nature of the ferrocene cyclopentadienyl rings at 360 K and the symmetry requirement that the principal axis of the ferrocene molecule must be placed perpendicular to the *a* axis are then interpreted as resulting from a dynamic disordering between *two* orientations of each ferrocene molecule that are related by the 2-fold axis through the iron atom. The ferrocene molecule in the structure at 148 K is in an almost eclipsed conformation (similar to the conformations found in crystalline forms of ferrocene[2]). Its principal axis is oriented at 78.4° to the crystallographic *a* axis. As the temperature increases this angle (as judged from the centroids of the adp ellipsoids) increases

(30) Dunitz, J. D.; Schomaker, V.; Trueblood, K. N. *J. Phys. Chem.* **1988**, *92*, 856−867.

(31) Ehrenfest, P. *Proc. Amsterdam Acad.* **1933**, *36*, 153.

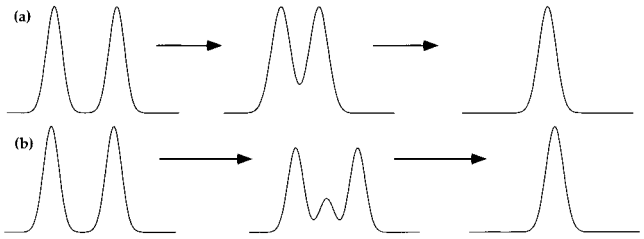

Figure 6. Schematic NMR spectra representing the progress of a transformation of a system from a phase with two distinct environments for a spin to one with a single environment for the spin: (a) where there is a gradual crystallographic change from one phase to the other, and (b) where there is a nucleation and growth of the product phase within the original phase.

to 79° at 200 K and 80.9° at 294 K, and in the single position interpretation of the 360 K $P22_12_1$ structure is constrained to be 90° by the 2-fold symmetry element. With the realization that the apparent eclipsed conformation is really a time-average structure, the transition, which might at first sight appear to relate to a change of *orientation* of the ferrocene molecule with respect to the DCA host, is recognized as actually being due to an *order−disorder* phenomenon. The X-ray data do not allow differentiation between a disordered model for the 360 K structure and an ordered model with (unacceptably) high thermal motion for the ferrocene molecules.

On heating from 300 to 350 K, the single-crystal XRD pattern shows a gradual decrease in intensity of reflections that are forbidden by the symmetry of the crystal structure of the high-temperature phase. This is consistent with an order−disorder transition, occurring when a degree of motion of one of the constituents increases significantly. Such transitions are often second-order thermodynamically and are considered to occur by a mode softening which causes a small cooperative displacement of molecules in the crystal, leading to a change in the crystallographic space group.[32,33] The XRD observations clearly support DSC evidence for a second-order transition

For a second-order phase transition, the NMR spectrum is expected to evolve gradually through the transformation regime from that typical of one phase to that characteristic of the other, as shown schematically in Figure 6a. For this model the environments of the target methyl groups equivalence over the temperature range of the phase change (see Figures 3b and 4b) with the concomitant changes and equivalancing of the chemical shifts.

In contrast, first-order transitions often occur through a mechanism of random nucleation and subsequent growth at the phase boundary.[32] Nucleation lag appears to vary between crystallites;[33] therefore, over a transition region the NMR spectrum is a superposition, in varying ratios, of those spectra characteristic of low and high-temperature phases. This is illustrated in Figure 6b, where the new phase is seen to "grow into" the previous phase. For this scenario single-crystal XRD detects the new phase when the domain size is large enough to generate Bragg peaks[34] and, when these domains start to dominate, the Bragg scattering from the original phase will be lost. Thus, most such transitions appear "sharp" by XRD.

We have examined the ^{13}C CP/MAS NMR spectra in greater detail to explore further the phenomenology of the phase transformation of **1**. The C21 and C19 DCA methyl resonances show the greatest changes during the transition and were selected for line shape fitting with both a 2-peak model (Figure 6a) and a 3-peak model (Figure 6b), from which values of chemical shift, line shape, line width, and intensity were obtained as a function of temperature. In addition, the line shapes were fit on the assumption of exchange broadening and coalescence on an equi-populated 2-site activated exchange model. All models can produce superficially acceptable fits to the experimental spectra.

This last proposal can be eliminated experimentally. Satisfactory fits on the activated exchange model require the chemical shifts of the two "static" peaks to move toward each other with increase in temperature, independently of the exchange process. A ^{13}C CP/MAS 2D-exchange NMR experiment with a mixing time of 1 s was performed at 318 K because an activated exchange process should show magnetization transfer effects at lower temperatures than the coalescence phenomena. Significant cross-peaks are predicted from the projected exchange rate calculated from the exchange-broadened line-shape simulations. Careful inspection of the 2D spectrum shows no evidence at all for cross-peaks, and we conclude that an exchange process between the two DCA molecule types does not cause the transformation of the NMR spectrum. Furthermore, on this model there is an expectation that the XRD determined adp ellipsoids would be elongated perpendicular to the DCA sheets but such an elongation is not observed.

The 3-peak model was rejected for two principal reasons. First, in the middle of the transition region (~327 K), the two peaks characteristic of the low-temperature phase have in comparison very different line widths, line shapes, and intensities in the fits.[35] Second, the fit parameters of each peak in the 3-peak model do not vary smoothly with temperature. In particular the intensity of the peak characteristic of the high-temperature form does not grow consistently with increase in temperature, but fluctuates, and the line width/shape varies erratically.

The simulations on the 2-peak model present regular changes in parameters through the transition region and resemble the experimental spectra very closely except at the midpoint of the transition, where there is a small residual intensity contribution between the resonances that cannot be simulated. As discussed, this additional intensity does not reflect a coherent third resonance, but we do not discount that an activated exchange process may be "switched-on" only as the difference between the different DCA molecule environments decreases (as judged by the increasingly similar chemical shifts). This would lead to some exchange-

(32) Rao, C. N. R.; Rao, K. J. *Phase Transitions in Solids*; McGraw-Hill: New York, 1978.

(33) Mnyukh, Y. V. *Mol. Cryst. Liq. Cryst.* **1979**, *52*, 163−200.

(34) Glusker, J. P.; Trueblood, K. N. *Crystal Structure Analysis: A Primer*, 2nd ed.; OUP: New York, 1985; pp 34−35. Amoros, J. L.; Amoros, M. *Molecular Crystals; Their Transforms and Diffuse Scattering*; Wiley: New York, 1968. Taylor, C. A.; Lipson, H. *Optical Transforms; Their Preparation and Application to X-ray Diffraction Problems*; Bell: London, 1964.

(35) This would be unexpected because of the similarity of the crystallographic environments that each peak reflects.

broadening effects without a lower-temperature magnetization transfer signature.[36]

The fit parameters for the 2-peak model for the C21 resonance are illustrated as a function of temperature in Figure 7. All the parameters plotted give an indicator that the transition "commences" at 305 K. The clearest is the line width ($\Delta\nu_{1/2}$), which between 260 and 305 K remains constant at ~10 Hz, after which it increases dramatically to a maximum of ~22 Hz by 325 K, before decreasing to 15 Hz by 360 K. The Lorentzian component of the line widths remains almost constant throughout and line width variation is Gaussian in origin; the Gaussian component of the Voigt line shape usually arises from the range of chemical environments present in the solid. The line width changes are therefore interpreted as indicating a disruption in the uniformity of the environment of the DCA molecules above 305 K, "peaking" at 325 K and an annealing process of the new form could account for the subsequent line width decreases on further temperature increase. The line width of 15 Hz at 360 K, in comparison with 10 Hz at 297 K, suggests that the annealing process may continue at still higher temperature.

The chemical shift of one of the peaks is largely independent of temperature over the range 260−300 K, but the other increases steadily by 0.3 ppm in the same range. Above 300 K the former peak's position becomes increasingly variable with temperature and the two peaks become closer in chemical shift. This is confirmed by the plot of the difference in chemical shift of the two peaks, which is linear with respect to temperature until ~300 K beyond which the gradient is much steeper. Most intriguingly, the plot of the mean chemical shift steadily increases by 0.2 ppm from 260 to 300 K, but above 300 K remains essentially the same to 360 K.

The chemical shift behavior could indicate two distinct stages to the transformation of **1** from the $P2_12_12_1$ to the $P22_12_1$ structure. In the first "pretransition" stage, the $P2_12_12_1$ structure undergoes temperature-dependent expansion in such a manner that one of the two DCA molecules changes its local environment more than the other. Beyond 300 K, transition phenomena are evident from NMR line widths and certain XRD spots first weaken in intensity. The chemical shifts indicate both molecules change environment increasingly dramatically with change in temperature. Finally, the line width data indicate a third stage of the process in which the $P22_12_1$ structure is continuing to develop its crystallinity above temperatures at which NMR chemical shifts and single-crystal XRD patterns suggest the transition is "complete".

These three different measures of the state of the system respond to the degree of order of the new phase in different ways. The NMR chemical shifts confirm the similarity by 345 K of the local environments of the previously independent DCA molecules. The XRD indicates the "long-range" ordering of that similarity by 360 K. The NMR line width/shape shows that the homogeneity of the local environments across a bulk crystalline sample is still developing even at 360 K. The transition on cooling may be described in an analogous manner.

(36) The exchange process will of course cease to exist when the DCA molecules are crystallographically identical, so no dipolar broadening or T_1 signature could be expected at higher temperatures.

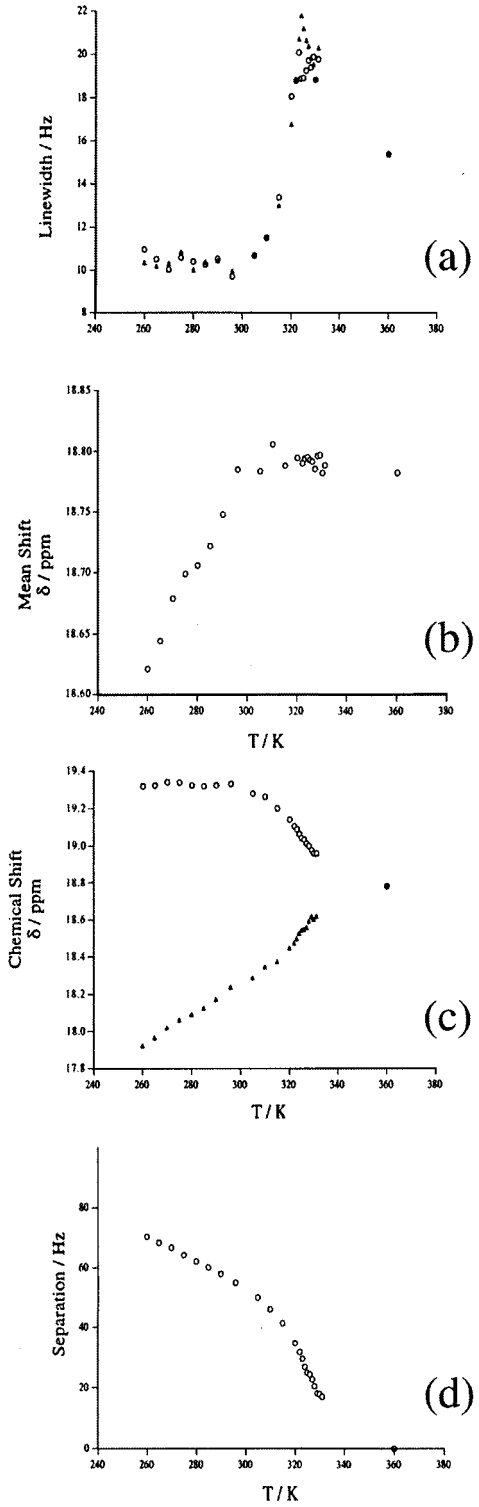

Figure 7. Temperature-dependent plots of (a) line width, (b) mean chemical shift, (c) chemical shifts, and (d) peak separation of the C21 methyl resonance of DCA in $(DCA)_2$:ferrocene (**1**), all obtained from line shape fits to a 2-peak model. The gap in the data from 335 to 360 K represents the inability to distinguish in terms of goodness-of-fit between a 2-peak and a 1-peak model. The uncertainty is probably because of the line-shape effects noted in the text and tentatively attributed to exchange-broadening. At 360 K, a 1-peak model is demonstrably sufficient to model the experimental spectrum.

The "trigger" for these changes appears to be the increasing/decreasing amplitude of the ferrocene molecular librations. The detailed study of the NMR parameters combined with the XRD observations thus

enables a plausible model for all stages of the transformation, including "pretransition phenomena" to be constructed and offers an interpretation of the meaning of the terms "onset", "peak", and "completion" of the transition.

Finally, given the conventional view of solid-state NMR being an ideal technique to study dynamic processes of molecules and XRD being the tool of choice for structural data, it is ironic that focusing on δ and $\Delta\nu_{1/2}$ for the DCA methyl carbon resonances in the ^{13}C CP/MAS NMR of **1** emphasizes the *host* structure, whereas XRD indicates more forcibly than NMR the part played in the transition by the orientation and reorientation of the ferrocene guest molecules.

Acknowledgment. This work was supported in part by EPSRC. M.M. gratefully acknowledges a postdoctoral research scholarship from the DFG. We thank Professor C. M. Dobson FRS for use of NMR facilities and useful discussions, Professor J. P. Glusker and Dr. H. L. Carrell for use of variable-temperature X-ray facilities. We thank M. Chronodopolos and Dr. J. M. Twyman for some early experiments in this project.

Supporting Information Available: Tables of the structure analyses, the final atomic coordinates, and anisotropic displacement parameters. This material is available free of charge via the Internet at http://pubs.acs.org.

CM990654A